

https://doi.org/10.1070/QEL17529

Dynamics of laser ablation of gold in melts of inorganic salts

M.I. Zhilnikova, I.I. Rakov, O.V. Uvarov, G.A. Shafeev

Abstract. **Nanosecond laser ablation of a bulk gold target in a melt of a sodium nitrate salt is investigated. It is shown that the form of plasma plumes on the target surface during ablation depends on the laser beam scan rate. The extinction spectra of sodium nitrate composites with gold nanoparticles during solidification is analysed.**

Keywords: *laser ablation, plasma, salt melts, nanofluids, nanocomposites.*

1. Introduction

Melts of inorganic salts are widely used in solar power engineering as heat-transfer agents and heat accumulators due to their high specific heat [1]. During daylight hours a melt circulates through a pipeline heated by concentrated solar light. In the absence of solar light the heat accumulated by the melt can be used to generate electric energy. This approach to solar energy conversion is believed to be one of the most efficient. If a melt contains nanoparticles, it is referred to as a nanofluid. It was found that even small additives of nanoparticles may increase significantly the specific heat [2–4], as well as to elevate the thermal diffusivity and thermal conductivity [5]. The initial materials for melts are nitrates of alkali metals, $NaNO_3$ and KNO_3, whose melting temperatures range from 300 to 350 °C. At the same time, salt melts are conducting ionic liquids transparent in the visible and near-IR spectral ranges.

Laser ablation of solids in liquids is a well-studied physical method of forming nanoparticles [6]. Conventional working liquids are such materials as water, alcohols, etc., which exist in the liquid state throughout the entire Earth's surface, except for the poles [6–9]. Salt melts are novel interesting media, in which nanoparticles can be generated by laser ablation. Laser ablation of some metals in salt melts was implemented for the first time in [10]. Gold nanoparticles were formed as a result of laser irradiation of a gold target in $NaNO_3$ and $NaNO_2$ melts at a temperature of about 320–340 °C; an ytterbium-doped fibre laser was used to this end. After laser ablation the morphology of Au and Al targets was studied, and the extinction spectra of solid nanocomposites salts with gold nanoparticles were registered.

In this paper, we report the results of experimental study of the extinction spectra of gold nanoparticles in a $NaNO_3$ liquid melt and demonstrate their evolution during melt solidification. In addition, the morphology of gold nanoparticles was investigated with a transmission electron microscope.

2. Results and discussion

The laser radiation source was an ytterbium-doped fibre laser with a wavelength of 1060–1070 nm and a pulse duration of 200 ns. The pulse repetition rate was 20 kHz. The laser fluence on the target surface amounted to ~7 J cm^{-2}. Note that melt splashing can be minimised at this energy density. The laser ablation of metals in salt melts is accompanied by plasma formation above the target (Fig. 1). Figure 1c shows how bubbles spread in the melt.

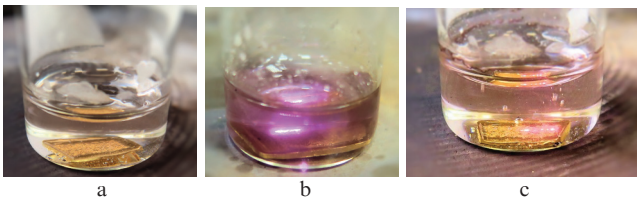

a b c

Figure 1. (a) Gold target in a $NaNO_3$ melt and (b, c) plasma plumes formed during laser ablation of the gold target at scan rates of (b) 100 and (c) 500 mm s^{-1}. The target length is 6 mm.

When the temperature of $NaNO_3$ exceeds its boiling point ($T > 380$ °C), this salt decomposes with the formation of $NaNO_2$ and oxygen release [9]:

$$2NaNO_3 \rightarrow 2NaNO_2 + O_2\,(\uparrow),$$

$NaNO_2$, in turn, is involved in the reactions

$$4NaNO_2 \rightarrow 2Na_2O + 4NO + O_2$$

or

$$4NaNO_2 + 2O_2 \rightarrow 4NaNO_3.$$

M.I. Zhilnikova Prokhorov General Physics Institute of the Russian Academy of Sciences, ul. Vavilova 38, 119333 Moscow, Russia; Moscow Institute of Physics and Technology (National Research University), Institutskii per. 9, 141701 Dolgoprudnyi, Moscow region, Russia;
I.I. Rakov, O.V. Uvarov Prokhorov General Physics Institute of the Russian Academy of Sciences, ul. Vavilova 38, 119333 Moscow, Russia;
G.A. Shafeev Prokhorov General Physics Institute of the Russian Academy of Sciences, ul. Vavilova 38, 119333 Moscow, Russia; National Research Nuclear University MEPhI (Moscow Engineering Physics Institute), Kashirskoe sh. 31, 115409 Moscow, Russia;
e-mail: shafeev@kapella.gpi.ru

Received 10 February 2021
Kvantovaya Elektronika **51** (4) 320–322 (2021)
Translated by Yu.P. Sin'kov

The gas atmosphere in a bubble on the target surface is determined by these reactions and, therefore, imposes some limitations on the possibility of forming metal nanoparticles of a number of metals by laser ablation in melts of the aforementioned salts. For example, the tantalum nanoparticles obtained by laser ablation in a $NaNO_2$ melt consist of tantalum oxide nanoparticles because of the presence of oxygen, whereas in the case of gold target purely metallic nanoparticles are obtained [10].

A specific feature of the plasma plumes observed in this study is their splitting along the laser beam path on the target surface. Indeed, a laser breakdown of a liquid may occur either in its vapour above the target [8] or around nanoparticles [11, 12]. However, at the chosen laser parameters, no breakdown occurs on nanoparticles because of the low laser radiation intensity (5×10^7 W cm^{-2}). A bubble containing $NaNO_3$ and O_2 vapour can be formed if the target temperature exceeds the melt boiling point. The $NaNO_3$ vapour pressure at this point is 1 atm. However, under the laser pulse, the target temperature exceeds the gold melting temperature, which leads to the formation of a bubble (filled with salt and oxygen vapour) on the target surface, after which a laser breakdown occurs.

Energy is consumed when a gas bubble is formed, as a result of which the target region around it is cooled. At the same time, if the laser beam scan rate is relatively high, the beam moves to the point whose temperature is below the melt boiling temperature (i.e., to the cold region). In this case, the target surface area located far from the formation point of previous bubble is heated. In other words, during laser breakdown bubbles are spaced at distances significantly exceeding the laser-beam diameter, due to which separate flares arise. For example, at an exposure of 1/60 s, the laser beam is displaced by 8 mm at a scan rate of 500 mm s^{-1}, whereas the plasma-plume size is less than 1 mm (Fig. 1c). At lower scan rates (100–300 mm s^{-1}), the plasma plume on the target surface is continuous because heat propagates (due to the thermal conductivity) in the target from the region exposed to the laser radiation to the unirradiated region. As a result, this bubble 'follows' the scanning laser beam (Fig. 1b). Thus, lower scan rates provide higher nanoparticle formation rates.

The extinction spectra of a liquid melt containing gold nanoparticles are of interest. These nanoparticles, generated by laser ablation in aqueous solutions, exhibit pronounced plasmon resonances in the visible spectral region [13, 14]. The extinction spectra were studied in the following way. Laser ablation of a gold target was performed in a glass Petri dish placed on an electric fryer. The thickness of $NaNO_3$ melt layer was several millimetres. After the end of ablation the dish was placed in a specially designed mounting, into which the light source and fibre detector of an OceanOptics spectrometer were also introduced (Fig. 2).

The melt extinction spectra were registered relative to a glass substrate. While the glass cell was cooled, the liquid melt with nanoparticles was solidified. A typical cooling time was 20–30 s.

Figure 3 shows the extinction spectra of gold nanoparticles in a $NaNO_3$ liquid melt and the nanocomposite Au–$NaNO_3$ during melt solidification. Spectra *1* and *2* correspond to a liquid melt containing gold nanoparticles. There is a distinguishable peak near 558 nm, which is reasonable to assign to the plasmon resonance of gold nanoparticles in liquid $NaNO_3$. The peak is red-shifted in comparison with the transverse plasmon resonance of gold nanoparticles formed

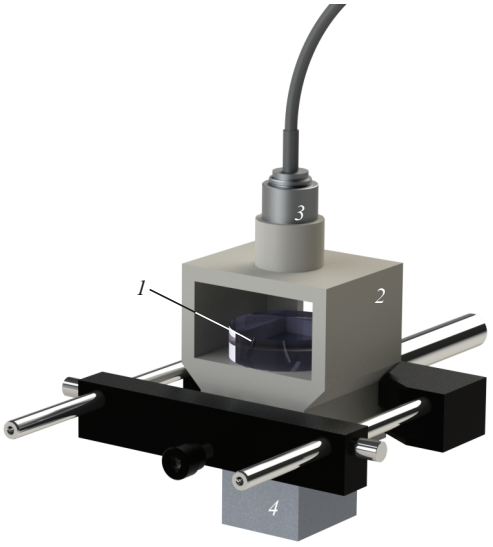

Figure 2. Fibre spectrometer unit for recording extinction spectra of nanoparticle-containing melts: (*1*) glass Petri dish; (*2*) mounting; (*3*) spectrometer optical fibre; (*4*) spectrometer light source.

by laser ablation in water [15, 16]. This shift is due to the large refractive index of liquid $NaNO_3$ as compared with H_2O. The plasmon resonance of gold nanoparticles formed during laser ablation of a target in a $NaNO_2$ melt is located near 445 nm. The distinction from the plasmon resonance in $NaNO_3$ is apparently due to the difference between the refractive indices of these two salts in the liquid phase.

During melt solidification the sample optical density increases in the entire visible spectral range, and scattering dominates over absorption. Crystallisation occurs nonuniformly throughout the melt bulk. This process begins at the cell periphery, because the heat removal is most intense in this region. The plasmon resonance of Au nanoparticles is retained at the same wavelength as in the solid phase. In addition, the solid-phase spectrum (*4*) contains a peak in the range of 850–900 nm. This peak was observed previously in the extinction spectrum of nanocomposite Au–$NaNO_3$ in the

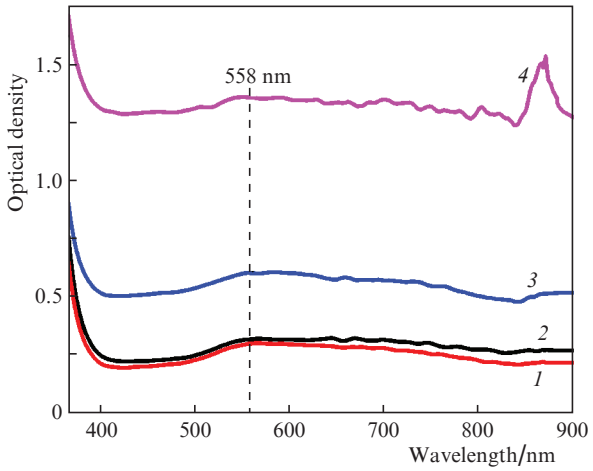

Figure 3. Extinction spectra of an Au–$NaNO_3$ nanocomposite during transition from (*1*) the liquid to (*4*) the solid phase upon cooling (the spectra were recorded relative to a glass substrate). The cooling times are (*1*) 0, (*2*) 10, (*3*) 20, and (*4*) 50 s.

solid phase [10]. It corresponds to the plasmon resonance of enlarged Au nanoparticles, which are formed during nanoparticle redistribution under the action of the solidifying melt. This effect is similar to the previously observed ordering of gold nanoparticles in a polymer nanocomposite [17].

After the dissolution of the solidified nanocomposite of a salt with gold nanoparticles, the latter are isolated from each other and do not form any aggregates. An image of gold nanoparticles is presented in Fig. 4.

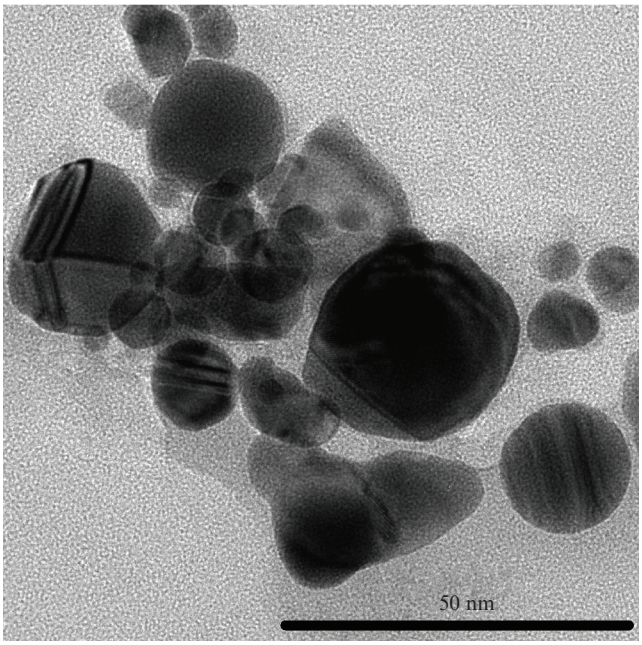

Figure 4. TEM image of gold nanoparticles formed by laser ablation of a target in a $NaNO_2$ melt, after dissolution of a solid nanocomposite in water.

It can be seen that the nanoparticle sizes range from several to several tens of nanometres; i.e., their sizes are close to those of nanoparticles obtained by gold ablation in aqueous media [18]. The shape of some particles differs from spherical. This can be explained by the plastic deformation of nanoparticles under the action of a solidifying melt.

3. Conclusions

Extinction spectra of gold nanoparticles in a liquid melt, obtained by laser ablation of a gold target in this melt, have been recorded for the first time. A plasmon resonance of nanoparticles is observed in the range of 545–560 nm, depending on the melt composition. The shape of plasma plumes on the target surface depends on the laser beam scan rate; at relatively high rates (about 500 mm s^{-1}), the plume becomes intermittent. After cooling the melt into a polycrystalline salt nanocomposite $Au–NaNO_3$, there arises a peak near 900 nm, which corresponds to the plasmon resonance of enlarged gold nanoparticles. After the salt matrix dissolution the nanoparticles are isolated and do not form any agglomerates.

Acknowledgements. This work was supported by the Russian Foundation for Basic Research (Grant Nos 18-52-70012 e-Asia and 20-32-70112-Stabil'nost') and RF President's Grant MD-3790.2021.1.2. This work was partly performed within the framework of National Research Nuclear University MEPhI (Moscow Engineering Physics Institute) Academic Excellence Project (Contract No. 02.a 03.21.0005). Also, we are grateful to Common Use Centre of GPI for TEM images.

References

1. Bauer T. et al., in *Molten Salts Chemistry* (Oxford: Elsevier, 2013) pp 415 – 438.
2. Svobodova-Sedlackova A. et al. *Renewable Energy*, **152**, 208 (2020).
3. Wei X. et al. *Renewable Energy*, **145**, 2435 (2020).
4. Zhou Y. et al. *Chem. Commun*., **52** (4), 811 (2016).
5. Myers P.D. et al. *Appl. Energy*, **165**, 225 (2016).
6. Shafeev G.A., in *Laser Ablation: Effects and Applications* (New York: Nova Science Publ., 2011) pp 191 – 225.
7. Kimura Y. et al. *Chem. Lett*., **36** (9), 1130 (2007).
8. Zhang D., Gökce B., Barcikowski S. *Chem. Rev.*, **117** (5), 3990 (2017).
9. González-Castillo J.R., et al. *Appl. Nanosci*., **7** (8), 597 (2017).
10. Zhilnikova M.I., Voronov V.V., Shafeev G.A. *Chem. Phys. Lett*., **755**, 137778 (2020).
11. Barmina E.V., Simakin A.V., Shafeev G.A. *Chem. Phys. Lett.*, **655–656**, 35 (2016).
12. Ortaç B., Şimşek E.U., Kurşungöz C., in *Laser Ablation – From Fundamentals to Applications* (InTech, 2017); DOI: 10.5772/intechopen.70594.
13. Amendola V., Meneghetti M. *Phys. Chem. Chem. Phys*., **11** (20), 3805 (2009).
14. Creighton J.A., Eadon D.G. *J. Chem. Soc. Faraday Trans.*, **87** (24), 3881 (1991).
15. Zhil'nikova M.I. et al. *Quantum Electron*., **50** (6), 608 (2020) [*Kvantovaya Elektron*., **50** (6), 608 (2020)].
16. Olejnik M. et al. *Acta Phys. Pol. A*, **122** (2), 346 (2012).
17. Barmina E.V. et al. *Phys. Wave Phenom*., **25** (3), 165 (2017).
18. Sylvestre J.-P. et al. *J. Phys. Chem. B*, **108**, 16864 (2004).